SAGO PALM 31-2: 71－78 (2024)

Phytolith Assemblages in Spined and Spineless Sago Palm (*Metroxylon sagu* Rottb.) Leaflets and Their Transport into Soil in Pangasugan, Leyte, Philippines

Masanori Okazaki[1]*, Mitsuhisa Baba[2], Keiji Nakaie[1], Masahiro Osada[1] and Marcelo A. Quevedo[3]

[1] Japan Soil Research Institute, Inc., 3-26-4, Yatocho, Nishitokyo, Tokyo 188-0001 Japan

[2] Kitasato University, 35-1, Higashi-Nijusanbancho, Towada, Aomori 034-8628 Japan

[3] Philippine Rootcrops Research and Training Center (PhilRootcrops), Visayas State University, Leyte, Philippines

* Corresponding author e-mail: japansoilco_okazaki@mbr.nifty.com

Abstract: To clarify the influence of the sago palm (*Metroxylon sagu* Rottb.) on the soil through phytolith formation, a transmitted-light microscope was used to determine the particle size, the number of conical projection spines (CPS), the vertex angle of the CPS, the length of the bottom of the CPS, and the height of the CPS of spheroid echinate phytoliths in spined and spineless sago palm leaflets and the soil surface from Pangasugan, Leyte, Philippines. The sago palms were transplanted from the Dulag area in the eastern part of Leyte in 2005, and leaflet samples were taken in 2016. The spined sago palm provided the smaller mean particle size, larger number of CPS, larger CPS vertex angle (131.8±12.5°), larger length of the bottom of CPS, and smaller height of CPS than those of the spineless sago palm. On the other hand, the CPS vertex angle of the spineless sago palm was 85.1±10.9°. Two angle peaks of CPS on the spheroid echinate phytoliths from 81 to 140° with one shoulder of 111 to 120° were found in the surface layer soil samples taken in 2019. Based on the CPS characteristics, it is concluded that the spheroid echinate phytoliths on the soil surface were transported from both the spined and spineless sago palm in the sago palm field of Pangasugan, Leyte.

Keywords: conical projection, spheroid echinate, spined, spineless

Introduction

Spined and spineless sago palms in the *Metroxylon* group were described by Nishikawa et al. (1979). In south central Seram, Mulk, Indonesia, the management of the great diversity of sago palms was sufficiently reported by Ellen (2006). Spined and spineless sago palms hold the same genetic information, although their apparent features are quite different (Ehara et al. 1997). Yamamoto et al. (2010), Pasolon (2015), Yamamoto et al. (2020), and Nurulhaq et al. (2022) determined that spined and spineless sago palms showed differences in starch production in Indonesia. It is deduced that the starch production of sago palms is related to Si uptake and phytolith formation because phytolith assemblages in sago palms are important to pathogen tolerance and animal resistance and have value for a mechanical barrier to strong wind.

On the other hand, phytoliths play a role in taxonomy (genus and species identification; wild and cultivated species differentiation; reconstruction of ancient floras, forests, and grass covers; and the determination of C3/C4 grasslands) (Bremond et al., 2004; Nawaz et al. 2019). Sago palms form phytoliths

(opal A) (Elzea et al. 1994, Curtis et al., 2019, Okazaki et al. 2020a), which provide historical evidence of human activity in the southern Pacific Ocean (Lentfer et al. 2021); however, phytolith analysis has advantages and disadvantages for the reconstruction of vegetation in Mediterranean areas (Bremond et al. 2004). Piperno et al. (2019) suggested that there was a strong relationship between people and palms in Amazonia. Moreover, Witteveen et al. (2022) explored how people and the environmental context have shaped the widespread occurrence of Amazonian palm species.

Meanwhile, Fishkis et al. (2010a, b) determined in laboratory and field study that the transportation rates of common reed (*Phragmites australis*) phytoliths applied to Haplic Cambisols and Stagnic Luvisols were different in the size and shape. In the field experiment, using a fluorescent labeling technique, the transportation rate for one year was found to be several cm from the surface for Cambisol (loamy sand soil) and Luvisol (silty loam soil) under an annual average precipitation of 1000 mm and an annual average temperature of 10.1 °C, respectively (Fishkis et al. 2010b).

Baba et al. (2020) showed the phytolith formation and its size distribution in spineless sago palm leaflets in Pangasugan, Leyte, Philippines. Okazaki et al. (2020a, b) exhibited the conical projection spines (CPS) of spineless sago palms using a transmitted-light microscope (TLM) and scanning electron microscope (SEM). The purposes of this study are to compare the phytolith assemblages derived from spined and spineless sago palms (*Metroxylon sagu* Rottb.) leaflets in Pangasugan, Leyte, Philippines, and to elucidate the transportation of sago palm phytoliths to the soil surface layer.

Fig. 1. Sago palm field in Pangasugan, Leyte, Philippines A: Spined sago palm (front row), B: spineless sago palm (trunk formation).

Materials and Methods

1. Sago palm leaflet samples

Spined and spineless sago palms, which were originally taken and transplanted from Dulag in 2005, were grown in Pangasugan, Leyte, Philippines (Fig. 1). The spined sago palm unidentified in the Visayas area was characterized by many medium spines on petiole, the generation of few suckers, and low growth. The spineless sago palm was found to have medium and fine spines on petioles, moderate sucker generation, and medium growth. The leaflet samples for phytolith analysis were collected from the third leaf from the bottom in 2016 (Fig. 2). The spined and spineless sago palms were examined 11 years after transplanting.

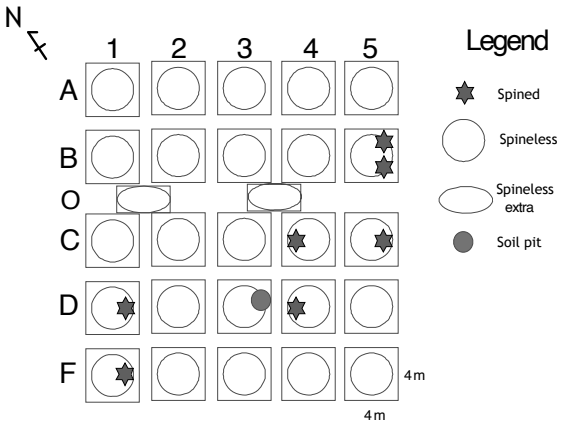

Fig. 2. Sago experimental field in Pangasugan, Leyte, Philippines

2. Soil samples

Surface soil (0–16.5 cm in depth) sampled by an auger in the Pangasugan sago palm field was taken from the intermediate point between spined and spineless sago palm growing sites in 2019 (Baba et al. 2021) and air-dried in Leyte, Philippines. The air-dried soil sample was sieved with a 2 mm mesh sieve and sent to Japan

for analysis of the phytoliths and primary minerals.

3. Extraction of phytoliths from sago palm leaflets and surface soil

In 2016, the leaflet samples were cut with a knife and scissors, air-dried, dried at 70°C for 24 hours in an oven, and heated at 500°C for 4 hours in an electric furnace. The ash sample was washed twice with distilled water and 0.001 mol/L HCl and collected via decantation using distilled water. The residue was sieved with a 0.045 mm sieve to remove large non-incinerated materials and washed with distilled water. Although almost all palm phytolith samples were in the fraction of less than 0.045 mm, fractions of more than 0.045 mm were also measured under a microscope to be certain.

The air-dried surface soil samples (< 2 mm) were treated with a 30% hydrogen peroxide solution to remove organic substances. Iron oxides that cover the phytolith surfaces were removed with a mixture solution (an 8 : 1 volume ratio of 0.3 mol/L sodium citrate to sodium bicarbonate) and 1 g of sodium dithionite for 15 min at 80 to 90 °C in a hot water bath (Baba et al. 2021). The soil samples, which were washed with 0.001 mol/L HCl and distilled water, were sieved with 0.250 and 0.045 mm sieves, respectively, and stored in plastic bottles (less than 0.045 mm and 0.045 mm to 0.250 mm fractions, respectively) separately after air drying. Fractions of less than 2 μm were excluded using a gravitational sedimentation method (sampling from 0 to 10 cm in depth after 8 hours).

4. Phytolith observation

Particles with diameters of less than 0.045 mm and those with diameters between 0.045 mm and 0.250 mm were mounted on a slide glass using a Matsunami MGK-S embedding agent (polystyrene). The phytoliths (ca. 100 grains) were counted under a polarized transmitted-light microscope (MT5000, Meiji Techno) at 400x magnification, and microscopic images were taken with a Cannon EOS Kiss X5 camera. The particle size of the CPS, CPS number, CPS vertex angle, length of the bottom of the CPS, and height of the CPS of spheroid echinate phytoliths in spined and spineless sago palm leaflets and the surface soil samples in Pangasugan were described (Okazaki et al., 2020a).

Results

1. Spined and spineless sago palm phytoliths in leaflets and the surface soil layer

Phytoliths in spined and spineless sago palms and the surface soil layer from Pangasugan are shown under a microscope (Figs. 3, 4, 5). Spheroid echinate phytoliths in spined and spineless sago palms line up in a row along parallel veins (Figs. 3, 4). Spined sago palms produced

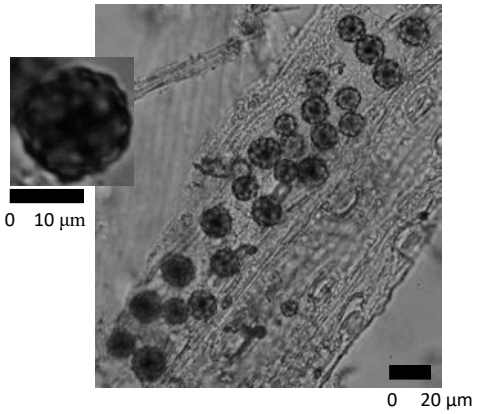

Fig. 3. Microscopic image of phytoliths in a spined sago palm leaflet

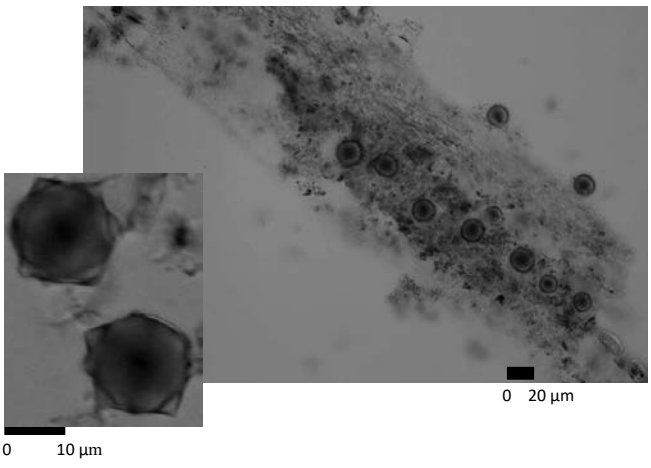

Fig. 4. Microscopic image of phytoliths in a spineless sago palm leaflet

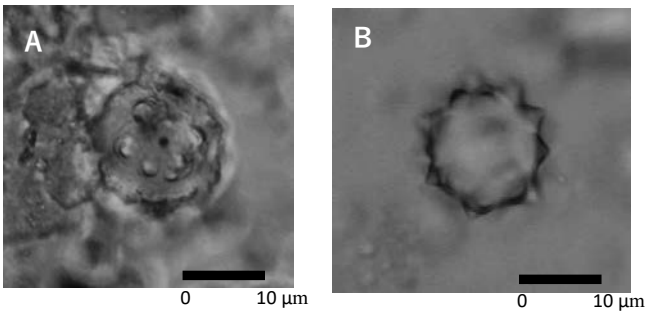

Fig. 5. Microscopic image of phytoliths in the surface soil layer
A: Spheroid echinate derived from a spined sago palm leaflet.
B: Spheroid echinate derived from a spineless sago palm leaflet.

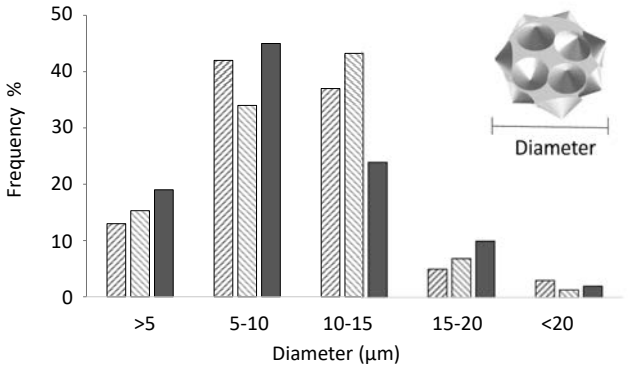

Fig. 6. Phytolith grain % in spined and spineless sago palm leaflets and the soil surface in the sago palm field, Pangasugan, Leyte, Philippines
Phytoliths in sago palm leaflets from spined sago palms.
Phytoliths in sago palm leaflets from spineless sago palms.
Phytoliths extracted from the soil surface layer (0–16.5 cm) in a soil pit.

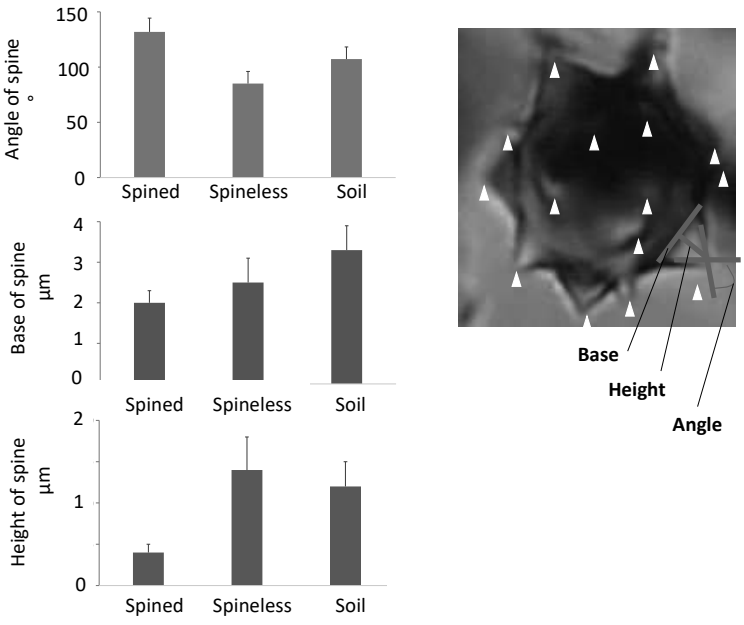

Fig. 7. Angles, bases, and heights of the conical projection spines in spined and spineless sago palm leaflets and on the soil surface in Pangasugan, Leyte, Philippines

spheroid echinate phytoliths —ranging from less than 5 μm to >20 μm—that were slightly smaller in diameter than those of spineless sago palms: the mean diameters of spined and spineless sago palm phytoliths were 9.15 and 9.99 μm, respectively (Figs. 3, 4). The CPS vertex angles of spined sago palm phytoliths were not sharper than those of spineless sago palm phytoliths, although the numbers of CPS were similar. Spineless sago palms have lager spheroid echinates, sharper CPS vertex angles, smaller lengths of the bottom of the CPS, and taller CPS than spined sago palms (Figs. 3, 4). Figure 5 shows two kinds of spheroid echinate phytoliths from the soil surface layer—large CPS angle (A) and small CPS angle (B) spheroid echinate phytoliths with similar diameters.

2. Size frequency percentages of phytoliths in spined sago palms, spineless sago palms, and the surface soil layer

The size frequency percentages of spined and spineless sago palm phytoliths are shown in Fig. 6. Spined sago palms had higher percentages of smaller spheroid echinate phytoliths, 5 to 10 µm (41%) and 10 to 15 µm (37%) in diameter. Phytoliths of spineless sago palms were 5 to 10 µm (33%) and 10 to 15 µm (43%) in diameter. The size frequency percentages of spheroid echinate phytoliths (Fig. 5) in the soil surface layer (0–16.5 cm) were found to be 44% (5 to 10 μm in diameter) and 10% (15 to 20 in diameter) (Fig. 6). Figure 7 shows the CPS angle, length of the bottom of the CPS, and height of the CPS in spined and spineless sago palms and the surface soil layer. The mean vertex angles of the CPS were 131.8 ±12.5° for the

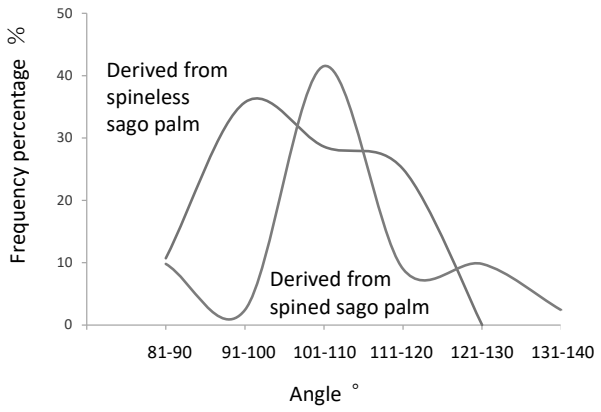

Fig. 8. Angle distribution of the conical projection spines in spheroid echinates on the soil surface at Pangasugan, Leyte, Philippines

spined sago palm, 85.1±10.9° for the spineless sago palm, and 107.3±10.9° for the surface layer soil. Figure 8 indicates that the angle distribution of the CPS in the spheroid echinate showed two large peaks at 91–100° with a shoulder at 111–120° (derived from the spineless sago palm) and 101–110° (derived from the spined sago palm). The mean lengths of the bottom of the CPS were 2.0±0.3 μm for the spined sago palm, 2.5±0.6 μm for the spineless sago palm, and 3.3±0.6 μm for the surface soil layer. The mean height of the CPS was 0.4±0.1 μm for the spined sago palm, 1.4±0.4 μm for the spineless sago palm, and 1.2±0.3 μm for the soil sample. Two contributors of sago palm phytoliths from the spined and spineless sago palms to the phytoliths in the soil surface layer might be determined by the characteristics of phytolith distribution.

Discussion

1. Phytoliths in spined and spineless sago palm leaflets in Pangasugan

Phytoliths are silica microfossils produced by many plants and can be preserved in soil. Arecaceae are known to be particularly prolific phytolith producers. Genes encoding proteins responsible for silicon transport control silicon accumulation, which is the result of an efficient symplastic pathway mediated by silicon influx and efflux transport mechanisms in the plasma membrane of root cells (Ma et al. 2006, Yamaji et al. 2008, Ma and Yamaji, 2015, Huisman et al. 2018). Rice (*Oryza sativa*) is able to take up silicic acid ($Si(OH)_4$ at a pH below 9) through Low silicon rice 1 and 2 (Lsi1 and Lsi2), which show high selectivity for silicic acid. Lsi1 belongs to the Nodulin 26-like intrinsic proteins (NIPs) subfamily in the aquaporin (AQP) family, while Lsi2 belongs to the ion transporter superfamily (Ma et al., 2006, Ma et al., 2007, Saitoh et al., 2021). However, studies of the silicon transporter of Arecaceae are quite limited. Bokor et al. (2019) reported on Si transporters in date palms (*Phoenix dactylifera*) and found that phytoliths in stigmata cells were present in roots, stems, and leaves. Phytolith formation in spined and spineless sago palm leaflets is not yet understood.

From this study, the spheroid echinate phytoliths in spined sago palm leaflets had slightly smaller diameters and wider angles than those in spineless sago palm leaflets. These facts might suggest that spheroid echinates with sharp CPS were provided to the spineless sago palm in the processes of genetic alterations during long-term cultivation.

2. Spheroid echinate phytoliths transported in the soil surface in Pangasugan

This study found that spheroid echinate phytoliths are transported from spined and spineless sago palm leaflets to the surface soil layer. The soil pore percentage is approximately determined by the soil particle size distribution—the percentages of clay, silt, and sand. The repetitive dry and moisture conditions and biological activities cause cracks and channels in the soil, which can percolate water and transport phytoliths. The diameters of cracks and channels are diverse and regulate the transportation of phytoliths. It is obvious that small-sized phytoliths (<5 μm and 5 to 10 μm phytoliths) also remained in the soil surface layer as a result of adsorption and the trapping of phytoliths on the surface of cracks and channels. Fishkis et al. (2010a, b) investigated common reed phytolith transport in soil at the laboratory and field levels using Haplic Cambisols and Stagnic Luvisols in

southern Germany. They determined that the weighted mean transport distances of phytoliths after one year were 3.99±1.21 cm for the Cambisol (texture: loamy sand) and 3.86±0.56 cm for the Luvisol (texture: silt loam), although the pore distributions of soils were not available. Albert et al. (2006, 2009) suggested an important loss of palm phytoliths based on deposition in the soils of Tanzania, which seemed to be related to the biostratinomic and post-depositional processes and to affect mostly larger phytoliths.

The biased preservation of the smaller spheroid morphologies was detected, due to the transport in soils, especially by the influence of phytolith sizes (Fishkis et al. 2010b). On the other hand, Liu et al. (2019) reported that phytoliths >30 μm in diameter with aspect ratios of >2 and phytoliths <20 μm in diameter with aspect ratios <2 were preferentially transported, as compared to phytolith >25 μm in diameter with aspect ratios of <2. They insisted that phytolith size and aspect ratio were important for phytolith transport in soil layers.

In the case of spheroid echinate phytoliths of sago palms, their aspect ratios are quite similar, so their size is much more important than their aspect ratio for their transport in the soil. From the comparative results of the production of phytoliths by spined and spineless sago palm leaflets and the phytoliths in the soil surface layer, the transport of phytoliths might depend on both water percolation through the cracks and channels and the adsorption of phytoliths on their surface charge. According to the results of Nguyen et al. (2021), the surface charge on rice phytoliths was detected to vary from slightly positive to negative (around -20 mmolc/kg at pH 6). The adsorption of phytoliths on the surface of cracks and channels in soils depends on the surface charges of both at an adsorption site. The isoelectric point of phytoliths from larch, elm, horsetail, ferns, and four kinds of grasses showed low pH$_{IEP}$ (0.9 to 2.2), which was very close to that of quartz or amorphous silica (Fraysse et al. 2009). The SiO- monodentate ligand on the phytolith surface is deduced to be adsorbed through various kinds of cations proposed from the soil.

In this study, the percentage of 10–15 μm spheroid echinate phytoliths in the soil surface layer was less than those in spined and spineless sago palm leaflets, which were deduced to be percolated to the subsurface layers with percolating water. On the other hand, spheroid echinate phytoliths <5 μm may easily remain on the surface of cracks and channels. Therefore, these results did not coincide with the results of Fishkis et al. (2010b).

The soil erosion and sedimentation rates at the foot of Mt. Pangasugan, Leyte (coconut monocropping, bryophyte and intact forest) were from 116 to 176 cm/year (Aureo 2018). However, there is no information regarding soil sedimentation at the Pangasugan experimental sago field. Aside from soil erosion and sedimentation, Patterer et al. (2020) looked at the phytoliths with signs of surface corrosion and dissolution that might correspond to the alkalinity of the environment. Although high alkalinity conditions (Kato et al. 1976) can result in a high degree of dissolution with fragmented and/or dissolved phytoliths and an important amount of silica debris (Kondo and Sase 1986), it is not strongly reflected in the phytolith assemblages in the Pangasugan surface soil at a pH of 6.4. It is unlikely that the difference in the CPS vertex angle and the length of the bottom of the CPS of spined and spineless sago palm leaflets is caused by the dissolution at the surface soil pH in Pangasugan (Lina et al. 2008), because the dissolution rate of SiO_2 decreases from pH 7 as the pH is lowered (Fujimoto 1991).

References

Albert, R. M., M. K. Bamford and D. Cabanes 2006 Taphonomy of phytoliths and macroplants in different soils from Olduvai Gorge (Tanzania) and the application to Plio-Pleistocene palaeoanthropological samples. Quaternary International 148, 78-94.

Albert, R. M., M. K. Bamford and D. Cabanes 2009

Palaeoecological significance of palms at Olduvai Gorge, Tanzania, based on phytolith remains. Quaternary International 193, 41-48.

Aureo, W. A. 2018 Evaluation of soil erosion and sedimentation processes of Pangasugan watershed in Baybay, Leyte, Philippines. European Journal of Research 11-12, 156-166.

Baba, M., M. Okazaki, K. Nakaie, T. Momose, M. A. Quevedo and S. B. Lina 2020 Phytoliths in the sago palm (*Metroxylon sagu* Rottb.) from Pangasugan, Leyte, Philippines. Sago Palm 28, 5-11.

Baba, M., M. Okazaki, K. Nakaie, M. A. Quevedo and Ma K. L. Aban 2021 Historical evidence of sago palm (*Metroxylon sagu* Rottb.) cultivation in Leyte, Philippines - Phytolith assemblages in soil Sago Palm 29, 1-13.

Bokor, B., M. Soukup, M. Vaculik, P. Vd'ačný, M. Weidinger, I. Lichtscheid, S. Vávrová, K. Šoltys, H. Sonah, R. Deshmukh, R. R. Bélanger, P. J. White, H. A. El-Serehy and A. Lux 2019 Silicon uptake and localisation in date palm (*Phoenix dactylifera*) - A unique association with sclenchyma. Frontiers in Plant Sciences 10 (988), 1-17.

Bremond, L., A. Alexandre, E. Véla and J. Guiot 2004 Advantages and disadvantages of phytolith analysis for the reconstruction of Mediterranean vegetation: an assessment based on modern phytolith, pollen and botanical data (Luberon, France). Review of Palaeobotany and Palynology 129, 213-221.

Curtis N. J., J. R. Gascooke, M. R. Johnston and A. Pring 2019 A review of the classification of opal with reference to recent new localities. Minerals 9, 1-20.

Ehara, H., S. Kosaka, T. Hattori, O. Morita 1997 Screening of primers for RAPD analysis of spiny and spineless sago palm in Indonesia. Sago Palm 5, 17-20.

Ellen, R. 2006 Local knowledge and management of sago palm (*Metroxylon sagu* Rottboell) diversity in south central Seram, mulku, eastern Indonesia. Journal of Ethnobiology 26, 258–298.

Elzea, J. M., I. E. Odom and W. J. Miles 1994 Distinguishing well ordered opal-CT and opal-C from high temperature cristobalite by x-ray diffraction. Analytica Chimica Acta 286, 107-116.

Fishkis, O., J. Ingwersen, M. Lamers, D. Denysenko and T. Streck 2010a Phytolith transport in soil: A laboratory study on intact soil cores. European Journal of Soil Science 61, 445-455.

Fishkis, O., J. Ingwersen, M. Lamers, D. Denysenko and T. Streck 2010b Phytolith transport in soil: A field study using fluorescent labelling. Geoderma 157, 27-36.

Fraysse, F., O. S. Pokrovsky, J., Schott and J-D. Meunier 2009 Surface chemistry and reactivity of plant phytoliths in aqueous solutions. Chemical Geology 258, 197-206.

Fujimoto, K. 1991 Rate and mechanism of dissolution of silicate minerals into aqueous solution - Characterization of mineral-aqueous solution interface, Mining Geology 41, 163-172. (in Japanese)

Huisman, S. N., M. F. Raczka and C. N. H. McMichael 2018 Palm phytoliths of mid-elevation Andean forests. Frontiers in Ecology and Evolution 6 (193).

Kato, Y., T. Matsui and I. Yamane 1976 Genesis and degradation of soils. Urban Kubota 13, 20-41. (in Japanese)

Kondo, R. and T. Sase 1986 Opal phytoliths, their nature and application. The Quaternary Research 25, 31-63. (in Japanese)

Lentfer, C.J., A. Crowther and R. C. Green 2021 The question of early Lapita settlements in remote Oceania and reliance on horticulture revisited: New evidence from plant microfossil studies at Reef/Santa Cruz, south-east Solomon Islands. Technical Reports of the Australian Museum Online 34, 87-106.

Lina, S. B., M. Okazaki, S. D. Kimura, S. Matsumura, M. Igura, M. A. Quevedo, A. B. Loreto and A. M. Mariscal 2008 Ammonium nitrogen releasing from kaolin-dominant soil in Leyte of the Philippines. Pedologist 52, 107-117.

Liu, L-D., D-H. Li, D-M. Jie, H-Y. Liu, G-Z. Gao and N-N. Li 2019 Translocation of phytoliths within natural soil profiles in northeast China. Frontiers in Plant Science 10, Article 1254 1-15.

Ma, J. F., K. Tamai, N. Yamaji, N. Mitani, S. Konishi, M. Katsuhara, M. Ishigura, Y. Murata and M. Yano 2006 A silicon transporter in rice. Nature 440, 688-691.

Ma, J. F., N. Yamaji, N. Mitani, K. Tamai, S. Konishi, T. Fujiwara, M. Katsuhara and M. Yano 2007 An efflux transporter of silicon in rice. Nature 448, 209-212.

Ma, J. F. and N. Yamaji 2015 A cooperative system of silicon transport in plants. Trends in Plant Science 20, 435-442.

Nawaz, M. A., A. M. Zakharenko, I. V. Zemchenko, M. S. Haider, M. A. Ali, M. Imtiaz, G. Chung, A. Tsatsakis, S. Sun and K. S. Golokhvast 2019 Phytolith formation in plants: From soil to cell. Plants 8 (249), 1-38.

Nguyen, A. M., C. T. Tran, Van T. Nguyen, T. T. T. Vu, L. N. Nguyen, S. Dultz and M. N. Nguyen 2021 Effects of rice-straw derived phytoliths on the surface charge properties of paddy soils. Geoderma 400, 112534.

Nishikawa, G., K. Oda and H. Suganuma 1979 Botanical description of sago palm. Japanese Journal of Tropical Agriculture 23, 123-130.

Nurulhaq, M. I., M. H. Bintro and Supijatno 2022 Morphology and starch production potential of sago palm found in Village Haripau, East Mimika Subdistrict, Mimika, Papua Province, Indonesia. Journal of Tropical Crop Science 9, 31-38.

Okazaki, M., M. Baba, T. Momose, M. A. Quevedo and M. K. L. Aban 2020a Conical projection measurement of sago palm (*Metroxylon sagu* Rottob.) Phytoliths in Leyte, Philippines. Sago Palm 29, 22-28.

Okazaki, M., M. Baba, T. Momose, M. A. Quevedo and M. K. L. Aban 2020b Phytolith assemblages in sago palm (*Metroxylon sagu* Rottb.) leaflets. Sago Palm 28, 35-48.

Pasolon, Y. B. 2015 Environment, growth and biomass production of sago palm (*Metroxylon sagu* Rottb.): A case study from Halmahera, Papua and Kendari. IJSTAS 2, 97 -104.

Patterer, N. I., D. M. Kröhling and A. F. Zucol 2020 Phytolith analysis in Quaternary fluvial deposits (El Palmar Formation-Late Pleistocene) of the Uruguay River valley, Entre Ríos province, Argentina. Journal of South American Earth Sciences 100 (102542), 1-13.

Piperno, D. R., C. N. H. McMichael and M. B. Bush 2019 Finding forest management in prehistoric Amazonia. Anthropocene 26, 100211.

Saitoh, Y., N. Mitani-Ueno, K. Saito, K. Matsuki, S. Huang, L. Yang, N. Yamaji,H. Ishikita, J-R. Shen and J. F. Ma 2021 Structural basis for high selectivity of a rice silicon channel Lsi1. Nature Communications 12 (6236), 1-14.

Witteveen, N. H., C. E. M. Hobus, A. Philip, D. R. Piperno and C. N.H. McMichael 2022 The variability of Amazonian palm phytoliths. Review of Palaeobotany and Palynology 300, 104613.

Yamaji, N., N. Mitani and J. F. Ma 2008 A transporter regulating silicon distribution in rice shoots. Plant Cell 20, 1381-1389.

Yamamoto, Y., F. S. Rembon, K. Omori, T. Yoshida, Y. N. Nitta, Y. B. Pasolon and A. Miyazaki 2010 Growth characteristics and starch productivity of three varieties of sago palm (*Metroxylon sagu* Rottb.) in southeast Sulawesi, Indonesia. Tropical Agriculture and Development 54, 1-8.

Yamamoto, Y., T. Yoshida, I. Yanagidate, F. J. Polonaya, W. A Siahaya, F. S. Jong, Y. B. Pasolon, A. Miyazaki, T. Hamanishi and K. Hirao 2020 Studies on growth characteristics and starch productivity of the sago palm (*Metroxylon sagu* Rottb.) folk varieties in Seram and Ambon islands, Maluku, Indonesia. Tropical Agriculture and Development 64, 125-134.